Validation of a CFD model simulating charge and discharge of a small heat storage test module based on a sodium acetate water mixture

Dannemand, Mark; Fan, Jianhua; Furbo, Simon; Reddi, Janko

Published in:
Energy Procedia

Link to article, DOI:
10.1016/j.egypro.2014.10.254

Publication date:
2014

Document Version
Publisher's PDF, also known as Version of record

Available online at www.sciencedirect.com

SciVerse ScienceDirect

Energy Procedia 00 (2013) 000–000

Energy Procedia

www.elsevier.com/locate/procedia

2013 ISES Solar World Congress

Validation of a CFD model simulating charge and discharge of a small heat storage test module based on a sodium acetate water mixture

Mark Dannemand*, Jianhua Fan, Simon Furbo, Janko Reddi

Department of Civil Engineering, Technical University of Denmark, Brovej 118, Kgs. Lyngby, DK 2800, Denmark

Abstract

Experimental and theoretical investigations are carried out to study the heating of a 302 x 302 x 55 mm test box of steel containing a sodium acetate water mixture. A thermostatic bath has been set up to control the charging and discharging of the steel box. The charging and discharging has been investigated experimentally by measuring surface temperatures of the box as well as the internal temperature of the sodium acetate water mixture through a probe located in the center of the steel box. The temperature developments on the outer surfaces of the steel box are used as input parameters for a Computational Fluid Dynamics (CFD) model. The CFD calculated temperatures are compared to measured temperatures internally in the box to validate the CFD model. Four cases are investigated; heating the test module with the sodium acetate water mixture in solid phase from ambient temperature to 52˚C; heating the module starting with the salt water mixture in liquid phase from 72˚C to 95˚C; heating up the module from ambient temperature with the salt water mixture in solid phase, going through melting, ending in liquid phase at 78˚C/82˚C; and discharging the test module from liquid phase at 82˚C, going through the crystallization, ending at ambient temperature with the sodium acetate water mixture in solid phase. Comparisons have shown reasonable good agreement between experimental measurements and theoretical simulation results for the investigated scenarios.

Selection and/or peer-review under responsibility of ISES

Keywords: Seasonal heat storage; sodium acetate trihydrate, phase change materials; thermal behavior; experiments; computational fluid dynamics

* Corresponding author. Tel.: +45 45 25 18 87
E-mail address: markd@byg.dtu.dk.

1. Introduction

Theoretical investigations have previously shown [1],[2],[3] that the solar fraction for solar heating systems can be improved significantly by the use of heat of fusion storages based on a sodium acetate water mixture with stable supercooling compared to solar heating systems with sensible and latent heat storages even under Danish climatic conditions. Calculations have shown that a solar heating system with a collector area of 36 m² can fully cover the yearly heat demand of a low energy house in Denmark if the solar heating system is equipped with a heat storage of 6 m^3 of sodium acetate water mixture which supercools in a stable way. Currently a development project is being carried out [4],[5],[6],[7] with the focus on developing such a heat storage. The storage is divided into a number of separate modules to optimize the system by allowing charge and discharge modules individually. The current module design is a flat steel tank with the salt water mixture enclosed in a chamber with heat exchangers integrated in the upper and lower surfaces. The inner height of the chamber containing the salt water mixture is 50-80 mm. In the current storage design each module contains 250-500 liters of salt water mixture. Previous experimental and theoretical Computational Fluid Dynamics investigations of prototype modules have shown deviations from the calculated to the measured values in some of the results [8].

This paper describes work done with a small 302 x 302 x 55 mm test steel box containing a sodium acetate water mixture. The focus is on the heating and cooling of the small test module and the behavior of the salt water mixture inside. The aim of this investigation is to compare theoretical CFD calculations to experimental measurements in order to validate the CFD model. A validated CFD model can be used to evaluate the suitability of differently designed heat storage modules.

Nomenclature

C_p specific heat, J/kg·K
h sensible enthalpy, J/kg
H enthalpy, J/kg
k thermal conductivity, W/m·K
L latent heat, kJ/kg
S source term
t time, s
T temperature, K
β liquid fraction, -
ρ density, kg/m^3
μ dynamic viscosity, kg/m·s
ΔH latent heat, J

2. Experimental setup

Three different scenarios are tested for charging: investigating only solid state salt water mixture by heating the module from 22˚C to 52˚C; investigating only liquid state salt water mixture by heating the module from 72˚C to 95˚C and investigating heating both solid and liquid state salt water mixture as well as the melting by heating the module from 22˚C to 78˚C/82˚C. For discharge the scenario of cooling from liquid state 82˚C to 19˚C solid state is investigated including the crystallization of the salt water mixture.

One 302 x 302 x 55 mm steel box containing a sodium acetate (58 %wt) and water (42 %wt) mixture with a melting point of 58˚C is heated up by placing it in a thermostatic bath containing water. The steel

box is filled with a sodium acetate water mixture in hot liquid state to obtain a complete filling of the test module with no air inside. The mass of the steel box is 4.626 kg and the mass of the salt water mixture filled into the box is 6.11 kg. The steel box has a material thickness of 2 mm. One side of the module has a filling neck for filling the module. Around the filling neck is a flange on which the lid is fixed. The filling neck has an inner diameter of approximately 40 mm. A brass container is located on the corner of the steel module which can be used to start crystallization of the salt water mixture if it supercools. The brass container is not relevant for this series of experiments and neglected.

Fig. 1. 302 x 302 x 55 mm steel module containing a salt water mixture.

In the center of lid a 170 mm long probe of stainless steel is fixed perpendicular to the plane of the lid. This places the tip of the probe in the center of the steel box when fastened. The probe has an outer diameter of 3 mm and a material thickness of 0.3 mm. A copper/constantan thermocouple (type TT) is placed inside the probe along with heat transfer compound to ensure maximum heat transfer from the probe to the thermocouple. A rubber gasket with a thickness of 4 mm is sealing the lid to the flange. 13 copper/constantan thermocouples (type TT) are fastened to the outer surfaces of the steel module with waterproof tape to measure the surface temperature of the steel module. Some inaccuracy of the surface temperature measurements are expected as the water temperature affects the measurements. Four sensors are placed on the top surface, two on the bottom surface, one on the side opposite from the lid and two on each of the remaining three sides. One last thermocouple is placed in the water. The measurements of the thermocouples are recorded every 2 seconds on an Agilent 34970A data logger.

A 600 mm x 400 mm x 215 mm plastic container constitutes the tub of the thermostatic bath. The tub is placed on 30 mm of Styrofoam insulation; the sides and top are covered with 75 mm of insulation to reduce heat losses and to keep a steady temperature inside the thermostatic bath. The water in the thermostatic bath is heated by a HETO Type 02 T 623 thermostat which includes a motor for stirring the water in the thermostatic bath to strive for uniform temperatures on all the surfaces of the steel module. Two pipes with valves are joined to the plastic container to work as inlet and outlet to allow for circulating cold water through the box to create an active discharge. The inlet and outlet are placed diagonally in the box for best circulation of water around the steel module during discharge. During charge the test module is covered with 35 mm of water and there is 60 mm of water from the bottom of the steel module to the bottom of the plastic container.

Fig. 2. Plastic tub for thermostatic bath with pipe connections and steel box.

To initialize the charge experiments the water in the thermostatic bath is heated to the desired end temperature; approximately 52˚C, 78˚C/82˚C and 95˚C without the steel module in the water. The steel module with the sensors attached is then placed in the hot water so that it is fully submerged. The module is placed on spikes to allow for water to be in contact with the entire bottom surface of the steel box. For the charge experiment with the salt water mixture only in liquid state the steel module is taken directly from an oven with a stable temperature of 72 ˚C. The charging runs until a stable temperature for the probe is reached in the center of the steel module. When a stable temperature is reached inside the module the thermostatic controller is turned off and the hot water in the thermostatic bath is emptied out and replaced with cold water from the tap. To simulate the discharge cold water is circulated through the plastic box with the lower pipe connection as the inlet and the pipe in the upper part of the thermostatic bath's box as an overflow outlet. During the discharge the steel module is covered with 20 mm of water. The discharge part of the experiment runs until the temperature measurement of the probe has stabilized.

Fig. 3 (a). Top view of thermostatic bath with steel box. (b) Thermostatic bath with lid and thermostatic controller.

During the charge/discharge the measured surface temperatures vary from one thermocouple to another due to local differences in thermal resistances between the steel box and the salt water mixture inside. For heating without a phase change the measured temperature differences are 2-4 K in the first 500 seconds and they are reduced to less than 1 K after 1000 seconds. For the charge from ambient temperature to 78˚C/82˚C the measured temperature differences are 2-3 K for the first 4-6000 seconds until the melting is complete and thereafter less than 1K. During the discharge initially the measured temperature differences are up to 10 K; reduced to less than 5 K after 1000 seconds and 1 K after 3000 seconds.

Due to the temperature dependent density of the salt water mixture the steel module deforms as it is heated up and cooled down. In the initial cold solid state the box has a relatively uniform thickness of about 55 mm. In the hot melted state the salt water mixture has expanded and the thickness of the steel box at the center is increased to about 65 mm with 55 mm near the sides. It is assumed that the box is full in the hot liquid state without air inside and the liquid salt water mixture is incompressible. The volume reduction of the salt water mixture from 82˚C to 22˚C is estimated based on the densities of the salt water mixture at the different phases and temperatures with the formulas (1) and (2). The estimated volume reduction of the salt water mixture between 82˚C and 22˚C is larger than the estimated volume change of the steel box by the deformation. This indicates that a vacuum is formed inside the steel box when in the solid state which is the initial state of the heating up experiments starting from 22˚C. It is assumed that the vacuum is formed in the part of the module facing upwards during solidification due to gravity forces. If the module is placed horizontally when the crystallization is started the vacuum is formed under the top surface. If the module is placed vertical when the crystallization is started the vacuum is formed by the side facing upwards. The vacuum will work as a thermal resistance on the face it is located for the heating in the first period until the salt water mixture has expanded enough to fill the module. Experiments with charging the module after crystallization at horizontal and at vertical position are carried out.

3. CFD model

A simplified model of the steel box is built using the commercial CFD code Ansys (Fluent) 14.5. The filling neck and lid are neglected. The probe is modelled as solid and is fixed on one of the side walls. Only the steel box including the enclosure, the probe and the salt water mixture inside is simulated. The measured surface temperatures of the steel module are used as input parameters for the CFD model. The charge of the steel module is simulated by assigning averages of the measured surface temperatures to the respective surfaces of the steel box in the CFD model as boundary conditions. The surface temperatures are defined in the model as functions of time by user defined functions (UDF). The UDFs for the surfaces are compared to the measured temperatures to ensure good agreement. The model is initialized at a uniform temperature representing the starting temperature of the experiment.

The mesh is shown in figure 4b below with the salt hydrate and the top and bottom surfaces suppressed. The mesh is denser near the outer surfaces, the transition from the steel to the salt water mixture and around the probe. The mesh has 437,462 elements and average skewness of 0.123.

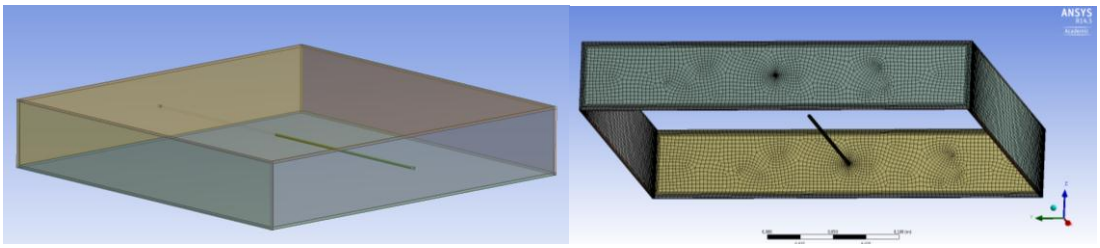

Fig. 4. (a) Geometry of the 302 x 302 x 55 mm steel box and probe in Ansys. (b) The mesh of the module with top and bottom surface and fluid suppressed.

Fluid flow in the box is calculated with a laminar model. Transient CFD calculations are performed with an initially standstill module (all fluid velocities are zero) and a uniform temperature. The PRESTO and second order upwind method are used for the discretization of the pressure and the momentum equations respectively. The SIMPLE algorithm is used to treat the pressure-velocity coupling.

During charge of the module, phase transitions of salt water mixture between solid and liquid phase will have a significant influence on the heat transfer in the module. The enthalpy-porosity method is used to calculate melting and crystallization of the salt water mixture. In the enthalpy-porosity method, the interface between the solid and liquid phase is not tracked explicitly. Instead, a quantity called the liquid fraction, which indicates the fraction of the cell volume that is in liquid form, is associated with each cell in the domain. The liquid fraction is computed every iteration, based on an enthalpy balance. The energy equation is written as [9]:

$$\frac{\delta}{\delta t}(\rho H) + \nabla \cdot (\rho \vec{v} H) = \nabla \cdot (k \nabla T) + S$$

Where ρ is density, kg/m^3; ν is fluid velocity vectors, m/s. S is Source term.

The enthalpy H of the salt water mixture, kJ/kg; consists of sensible enthalpy, h and latent heat, ΔH.

$$H = h + \Delta H$$
$$h = h_{ref} + \int_{T_{ref}}^{T} C_p \, dT$$

Where H is the enthalpy, kJ/kg; C_p is the specific heat of salt water mixture; T is the temperature in K.

The latent heat is calculated by a product of the liquid fraction and the latent heat of the material.

$$\Delta H = \beta L$$

Where L is the latent heat of salt water mixture; β is the liquid fraction, -.

The liquid fraction is 1 when the salt water mixture temperature is higher than the melting point temperature, while it is 0 if the salt water mixture temperature is lower than the melting point temperature. In this way, melting and crystallization of salt water mixture during the charge of the module are considered.

The density of the mixture of 42% (weight) water and 58% (weight) sodium acetate is and its temperature dependency is adapted from Lane [10] and Fan [8]. Specific heat and thermal conductivity are adapted from Araki [11]. Dynamic viscosity is adapted from Inagaki [12]. Latent heat of the 42% (weight) water and 58% (weight) sodium acetate is assumed to L = 240 kJ/kg [13].

Density, [kg/m^3]: $\rho = 1523 - 0.780 \cdot T$ (1)

Thermal expansion coefficient, [1/K]: 0.000512

Specific heat, [J/(kgK)]: $C_p = 1594 + 4.33 \cdot T$

Thermal conductivity, [W/(mK)]: $k = -2.72 + 0.0214 \cdot T - 3.63 \cdot 10^{-5} \cdot T^2$

Dynamic viscosity, [kg/(ms)]: $\mu = 0.3673 - 0.001943 \cdot T + 2.592 \cdot 10^{-6} \cdot T^2$

where T is fluid temperature, [K].

The following properties of the solid salt water mixture and their dependences on temperature are used: Specific heat and thermal conductivity adapted from Araki [11]. Density from Lane [10].

Density, [kg/m^3]: 1450 (2)

Specific heat, [J/(kgK)]: $C_p = 1017 + 3.50 \cdot T$

Thermal conductivity, [W/(mK)]: $k = 0.60$

where T is fluid temperature, [K].

The steel wall has a thermal conductivity of 60 W/K and a specific heat of 500 J/kgK. The density of the steel is assumed to be 9590 kg/m^3 based on the mass of the steel box and the volume of the steel in the CFD model.

For the heating up the solid salt water mixture from 22˚C to 52˚C a resistance of 0.0476 m^{2}K/W corresponding to a vacuum of 1/3 mm is assigned to the inner top surface of the steel box. This represents the vacuum related the contraction of the salt water mixture in the cold solid state. For the heating from 72˚C to 95˚C and from 22˚C to 78˚C/82˚C no resistances are assigned. The geometry of the steel box and the volume of the fluid are assumed to be constant regardless of the temperature level.

4. Results and discussion

The temperature measured in the center of the steel box by the probe is compared to the simulated temperature of the probe tip in the CFD model.

Figure 5 shows good agreement between the development of the measured probe temperature and the simulated temperature of the probe tip for the heating from 22°C to 52°C in the solid state. A contact thermal resistance for the heat transfer is applied to the top inner surface of the steel box representing a small vacuum in the top of the box. Simulating the experiment without the contact resistance would lead to a faster heating of the probe tip.

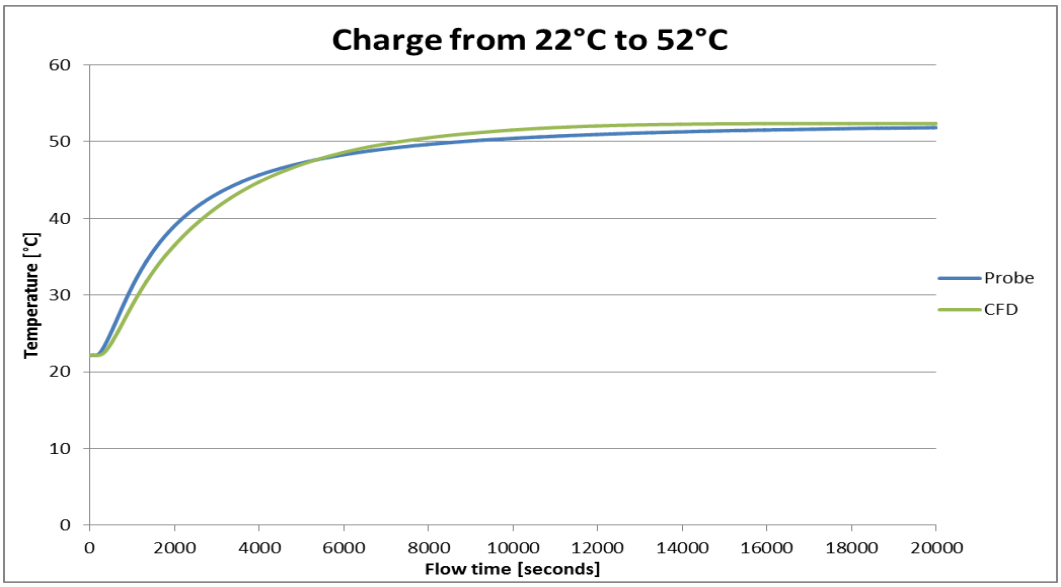

Fig. 5. Comparison of probe measurement and simulation tip temperature development for heating from 22°C to 52°C.

Figure 6 shows good agreement between the development of the measured probe temperature and the simulated temperature of the probe tip in the case of heating the liquid salt water mixture from 72°C to 95°C without any resistances applied.

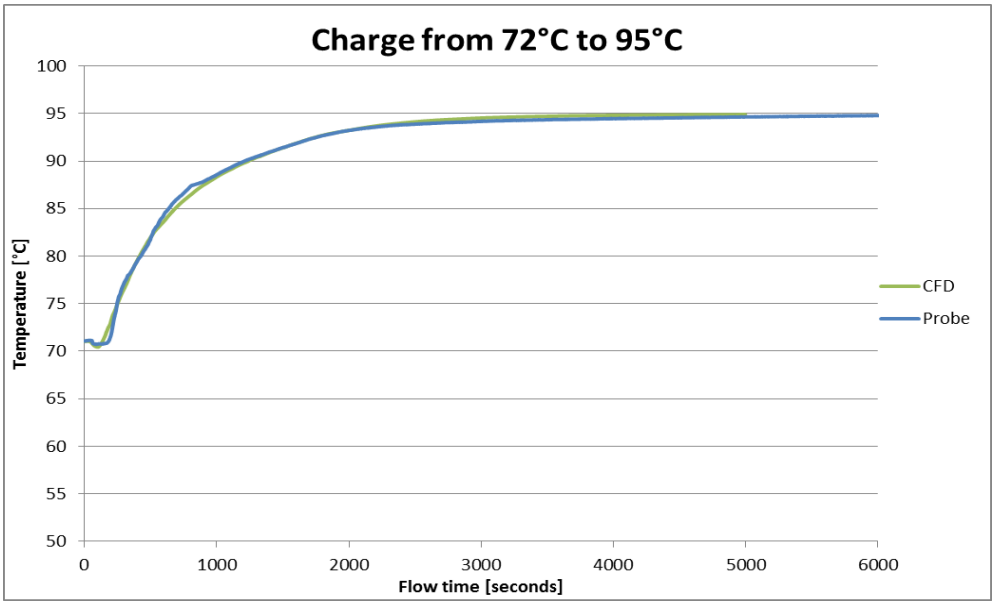

Fig. 6. Comparison of probe measurement and simulation tip temperature development for charging from 72°C to 95°C.

Figure 7 shows the temperature developments of the probe for the experimental setup compared to the simulated probe tip temperature development for two similar tests. (Probe1) Heating from 22°C to 78°C after crystallization of the salt water mixture with the module placed horizontally. (Probe2) Heating from 22°C to 82°C after crystallization of the salt water with the module placed vertical. It is assumed that for Probe1 a resistance caused by the vacuum on the top surface is reducing the heating rate compared to Probe2 where the vacuum is near the side and therefore has lower influence of the heating of the probe in the center. The end temperature for the two experiments differs with about 4K which partly causes the slower heating rate of Probe1 compared to Probe2. For each case the different boundary conditions are applied to the CFD model which gives the different results for the simulations CFD1 and CFD2. For both simulations no resistances are applied. The deviations between the experiment Probe1 and simulations CFD1 are much larger than the deviations between Probe2 and CFD 2. This supports the theory of vacuum forming inside the steel module resulting in a thermal resistance and reduced heating rate.

The deviations between the measured and simulated temperatures can also be influenced by the imprecise method of which the surface temperature of the box is measured. This can be an overestimation of the actual surface temperatures which are used as the boundary conditions for the CFD model.

It can be seen that the temperature of the sensor in the probe inside the steel box in the first part of the charging rises at a relative constant rate due to the thermal conduction in the salt water mixture from the hot outer surface through the salt hydrate to the probe. The curve flattens out and the heating rate of the probe decreases partly due to the thermal energy being absorbed by the phase change of the salt water mixture near the outer surfaces and partly because the temperature difference of the probe and the surface temperature of the steel box decrease. Considering no surface resistances on the upper surface, the last part of the salt water mixture that melts is in the middle part of the steel box where the sensor is located.

The last solid salt water mixture will be fixed in the center of the test module and not moving freely in the box because it surrounds the probe. When the part of the solid salt water mixture that is fixed to the probe comes loose it drops to the bottom of the steel box due to its higher density and the convection inside the steel box and around the probe is increased and the temperature of the probe increases rapidly when the warmer liquid near the surfaces are mixed with the just melted salt water mixture near the probe in the center.

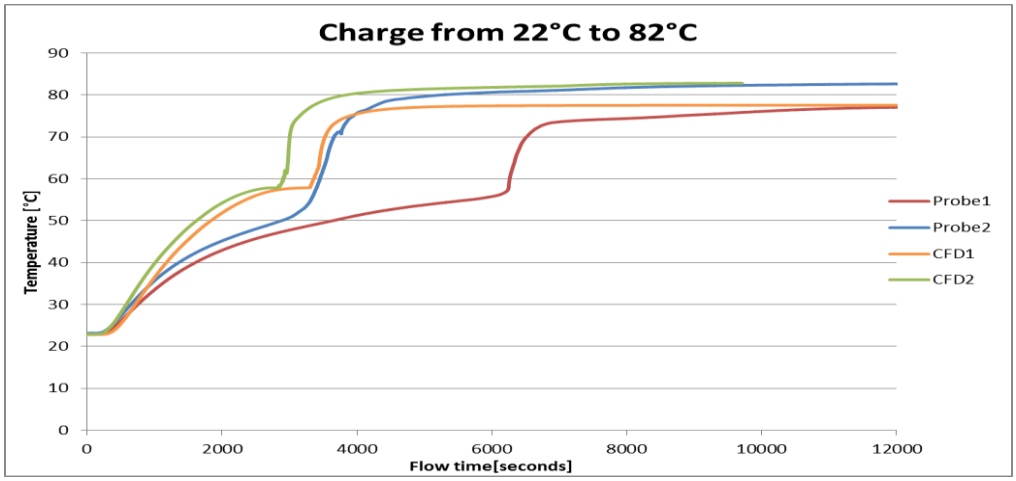

Fig. 7. Comparison of probe measurement and simulation tip temperature development for heating from 22°C to 82°C and 78°C.

Figure 8 shows the data for the discharge from 82°C to 19°C. The crystallization of the salt water mixture started spontaneous with only slight supercooling. The measured temperature development of the probe agrees well with the simulated probe tip temperature. The horizontal part of the curve indicates the release of the heat of fusion which for the measurement is slightly shorter than for the simulations. This can indicate that the latent heat of 240 kJ/kg used in the CFD model could be an over estimation.

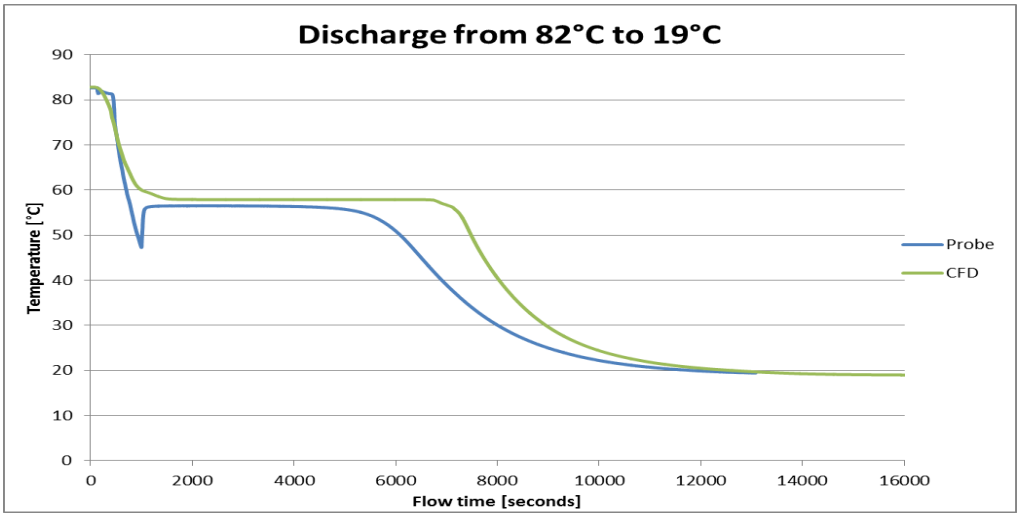

Fig. 8. Comparison of probe measurement and simulation tip temperature development for discharging from 82°C to 19°C.

5. Conclusion

Thermal experiments and CFD simulations have been carried out in order to investigate the behavior of a test steel module containing a salt water mixture and to validate the CFD model. Comparisons between measured temperatures for charging and discharging and temperatures calculated with a CFD model have shown good agreement. For heating of the salt water mixture without phase change the agreement between measurement and simulations are excellent. For the temperature developments through the phase change some deviations between measured and calculated temperatures are observed. More investigations are needed in order to understand the reasons for these differences.

The experimental investigations showed that orientation of the module when the salt water mixture crystalizes and the forming of vacuum in the rigid steel module can have a large effect on the heating rate of a module due to thermal resistances being created internally in the module by the vacuum. Considerations of rigidness and designs for full scale heat storages should be made to avoid lower heat transfer rates. Especially vacuum forming near the heat exchanger for the module can reduce the heat exchange capacity rate and reduce the efficiency of the storage system.

References

[1] J. Schultz and S. Furbo, “Solar heating systems with heat of fusion storage with 100% solar fraction for solar low energy buildings,” in ISES Solar World Congress 2007 Proceedings, 2007.

[2] S. Hirano and T. S. Saitoh, “Heat balance of long-term supercooled thermal energy storage,” Nihon Enerugi Gakkaishi/Journal of the Japan Institute of Energy, vol. 80, no. 11, pp. 1050–1059, 2001.

[3] S. Hirano and S. Takeo, “INFLUENCE OF OPERATING TEMPERATURE ON EFFICIENCY OF SUPERCOOLED THERMAL ENERGY STORAGE,” in IECEC 2002 Paper No. 20040, 2002, no. 20040, pp. 684–689.

[4] S. Furbo, J. Dragsted, J. Fan, E. Andersen, and B. Perers, “Experimental studies on seasonal heat storage based on stable supercooling of a sodium acetate water mixture,” ISES Solar World Congress 2011 Proceedings, 2011.

[5] S. Furbo, J. Fan, E. Andersen, Z. Chen, and B. Perers, “Development of Seasonal Heat Storage based on Stable Supercooling of a Sodium Acetate Water Mixture,” Energy Procedia, vol. 30, pp. 260–269, 2012.

[6] W. Van Helden, A. Hauer, S. Furbo, O. Skrylnyk, A. Ristić, S. Henninger, C. Rindt, F. Bruno, A. Lázaro, L. Luo, D. Basciotti, A. Heinz, R. Weber, I. Fernandez, J. Chiu, H. Zondag, R. Cuypers, J. Jänchen, and E. Lävemann, “Results of 4 years R & D in the IEA Task4224 on Compact Thermal Energy Storage : Materials Development for System Integration Task 4224.”

[7] T. Letz, E. Andersen, C. Bales, J. Bony, R. Heimrath, M. Haller, R. Haberl, J. Hadorn, D. Jaehnig, H. Kerskes, J. Schultz, R. Weber, and H. Zondag, “Performances of solar combisystems with advanced storage concepts Report A3 of Subtask A,” 2007.

[8] J. Fan, S. Furbo, E. Andersen, Z. Chen, B. Perers, and M. Dannemand, “Thermal Behaviour of a Heat Exchanger Module for Seasonal Heat Storage,” Energy Procedia, vol. 30, pp. 244–254, Jan. 2012.

[9] ANSYS 14.5 Help. Fluent Theory Guide: 18. Solidification and Melting // 18.4. Energy Equation

[10] G. Lane, Solar heat storage latent heat material Vol 2. CRC, 1986.

[11] N. Araki, M. Futamura, A. Makino, and H. Shibata, “Measurements of Thermophysical Properties of Sodium Acetate Hydrate,” International Journal of Thermophysics, vol. 16, no. 6, pp. 1455–1466, 1995.

[12] T. Inagaki and T. Isshiki, “Thermal Conductivity and Specific Heat of Phase Change Latent Heat Storage Material Sodium Acetate Trihydrate and Heat Transfer of Natural Convection in a Horizontal Enclosed Rectangular Container,” Kagaku Kogaku Ronbunshu, vol. 39, no. 1, pp. 33–39, 2013.

[13] R. Tamme, “Low Temperature Thermal Storage Using Latent Heat and Direct Contact Heat Transfer,” in 21st Intersociety Energy Conversion Engineering Conference, 1986.